ARTICLES

Vibrational and Photoionization Spectroscopy of Neutral Valine Clusters

Yongjun Hu*,†,‡ and Elliot R. Bernstein*,‡

MOE Key Lab of Laser Life Science & Institute of Laser Life Science, South China Normal University, Guangzhou 510631, P. R. China, and Department of Chemistry, Colorado State University, Fort Collins, Colorado 80523-1872

Received: February 10, 2009; Revised Manuscript Received: June 16, 2009

We report the first observation of infrared (IR) and mass spectra of neutral, aliphatic amino acid clusters: the example presented herein is for $(valine)_n$, $n = 2-5$. The clusters are generated in a supersonic expansion and their IR spectra are recorded in various fragment and $(valine)_{n-1}H^+$ ($n = 2-5$) mass channels. The ions are created by single photon ionization with a VUV laser at 118 nm (10.5 eV/photon) following IR absorption in the single photon energy range 2500−4000 cm^{-1}. Mass channels obviously associated with valine clusters lose intensity and mass channels associated with valine monomers gain intensity under IR irradiation. No free OH modes are identified in any of these spectra suggesting that for $(valine)_n$, $n = 1-5$, all the OH groups are hydrogen bonded. The infrared transition for the hydrogen bonded OH moiety appears as a very broad, shifted feature ca. 3000 cm^{-1} (∼2800 to ∼3200 cm^{-1}). Free and perturbed NH_2 modes can also be identified in the cluster spectra. CH modes ca. 3000 cm^{-1} can be identified and appear to be coupled to the shifted and broadened OH modes of the clusters. Fragmentation pathways for three $(valine)_2$ isomers under 118 nm ionization are proposed and discussed.

I. Introduction

Many details of the intrinsic properties of biomolecules are obscured by elements of the biological environment (e.g., solvents, other polymers, etc.). Reports in the literature show that the understanding of isolated amino acids, peptides, sugars, saccharides, and even their clusters can lead to unraveling the interactions, mechanisms, and essential features of the final structures for proteins, carbohydrates, and nucleic acids.[1] IR absorption spectroscopy can be a unique identifier of such component structures: absorption line widths, intensities, and energies can give direct information on the hydrogen bonding and other interactions that hold the larger biopolymer molecules together and control their higher order structures ("shapes"). IR absorption spectra of gas phase species can be obtained by ion- or fluorescence-dip spectroscopy,[2−5] a technique that has been applied to various systems, such as isolated or paired nucleobases,[6] amino acids with aromatic chromophores (phenylalanine and tryptophan),[7,8] and very recently the β-turn or helical peptide (aromatic) model systems.[9,10] Aromatic substituted sugars have also been accessed in this manner.[11] These studies have been performed using IR laser systems that cover the near- to mid-IR region (e.g., 2500−7000 cm^{-1}). In this range X−H (X = C, O, N) stretching vibrations can be probed and the results can provide insight into the conformational arrangements of the polymer building blocks, as transitions exhibit shifts in absorption intensity and energy, and line widths (interactions and mode couplings) change due to the presence of both intra- and intermolecular hydrogen bonding.

The work referenced above pertains to biological building block species that possess an aromatic moiety. The phenyl or indole aromatic moiety serves as a chromophore, through which two photon resonant ionization can be achieved to detect the vibrational mode excitation of the molecule in its electronic ground state. The ion state is then localized on the aromatic ring and is relatively weakly coupled to the (NH_2)CHCOOH amino acid ("back-bone") moiety. The restriction of such experiments to aromatic containing molecules arises from the fact that commercially available lasers are typically only tunable to ca. 200 nm and thus two photon absorption is required for ionization at ca. 9 eV ionization energy: this limitation would exclude systems such as simple sugars, saccharides, and the simplest, nonpolar, aliphatic amino acids from such ion- or fluorescence-dip experiments.[12]

In our present study, the ionization/detection step for IR vibrational absorption is through single photon ionization at 10.5 eV (118 nm). This energy is sufficient to ionize all amino acids and sugars directly. Clearly, the advantage of this approach is that the IR spectra of any (not just aromatic) amino acids, etc. and/or their clusters in the gas phase can be studied by IR plus VUV spectroscopy. Thereby, the structure and dynamics of such species can be investigated through analysis of their CH, OH, and NH modes, and vibrational overtones and combinations, in general. The ion in the present case is generated from the mixed lone pair nitrogen−oxygen orbital[13] that is the HOMO for the species, and this orbital is directly involved with the amino acid (NH_2)CHCOOH molecular moiety. While single photon ionization removes the requirement of an aromatic chromophore, it can have the drawback that it lacks the

* Corresponding authors. E-mail: E.R.B., erb@lamar.colostate.edu; Y.H., yjhu@scnu.edu.cn.
† South China Normal University.
‡ Colorado State University.

10.1021/jp901208f CCC: $40.75
Published on Web 07/08/2009

spectroscopic selectivity that resonant ionization can in some instances provide. Nevertheless, in some cases (e.g., aniline−methanol[13d]), the intermediate S_1 state employed for two photon resonance ionization may not be well resolved.

Cluster formation in a supersonic expansion provides the opportunity to study interactions between individual molecules:[14] some reports for biologically related nucleobases (base pairs) have appeared,[15−17] and a few reports on neutral clusters of amino acids and peptides are also available in the literature.[18] The latter clusters can be considered as model systems for β-sheets of protein structures and the building blocks of biological macromolecules (peptides and proteins), in general.

We have reported studies of radicals, alcohols, and acids in the past few years employing nonresonant, single photon ionization to detect IR absorption in both neutral and cationic states.[19] In these studies one does not typically detect the neutral cluster distribution due to fragmentation of monomers and multimers due to the ionization step and infrared absorption. Each of these fragmentation steps is different. As we have demonstrated for van der Waals clusters in general,[19,20] as well as other systems,[21] single VUV and EUV photon ionization leaves the system in the neutral (Franck−Condon) geometry with the vertical ionization energy (VIE). The excess ionization energy, that is, the photon energy above the VIE ($h\nu$ − VIE) is removed by the ionized electron in the form of kinetic energy. Such behavior has been characterized for a wide variety of cluster systems, such as $(H_2O)_n$, $(NH_3)_n$, M_m, and many others.[19,20] Where applicable, the same mass spectrum arises for 193, 118, and 46.9 nm ionization. The difference between the VIE and the adiabatic ionization energy (VIE-AIE) is vibrational energy in the monomer or cluster that can be employed to generate ion unimolecular reactions that initiate molecular and/or cluster fragmentation (i.e., VIE-AIE + ΔH_{react}).[19] The monomer, fragments, and cluster distribution detected by mass spectrometry are thus only related to the nascent, neutral cluster distribution. While determination of the neutral monomer/cluster distribution is interesting, it is not the main goal of these studies. Our emphasis, rather, is on the detection of the infrared spectra of monomers, dimers, etc. (to the extent it is experimentally possible) to learn about structure, binding, and interactions within these respective systems.

Introduction of IR radiation prior to the ionization step can have two different influences on the detected mass spectra. First, the absorbed IR photon(s) does not necessarily cause fragmentation of the molecule or clusters in the neutral ground electronic state (e.g., $h\nu_{IR} \lesssim$ cluster binding energy). In this case the energy added to the system can be employed to open or enhance or reduce fragmentation channels, which are created following the VUV single photon ionization step. Findings for other systems[19] show that new fragmentation channels are not opened by this IR/VUV excitation, rather different existing (VUV generated) channels are enhanced and/or depleted. Thus the IR absorption for monomers or clusters can be identified by detecting the absorption of the IR photons in the various mass channels observed. Second, absorbed IR photons can cause fragmentation of clusters prior to absorption of the VUV ionization photon. In these experiments, the IR photons precede the VUV ionizing photon by 10−50 ns, so intracluster vibrational redistribution of energy (IVR, ca. 1 ps) and vibrational predissociation of the clusters (VP, ca. 1 ps to 10 μs depending on cluster size and the number of absorbed IR photons) can fragment the clusters prior to the ionization step. Information concerning the nascent cluster distribution can thereby be compromised by this mechanism, but again the central issue is not this distribution: the central issue is the infrared spectra of the various species present in the sample. To the extent that cluster spectra are similar (e.g., all OH moieties are involved in hydrogen bonding, all CH moieties are not involved in intermolecular bonding, and some of the NH moieties are not involved in hydrogen bonding, etc.), then qualitative information can be generated concerning cluster structure and intermolecular interactions from the cluster IR spectra. In this experiment no new fragments are observed with the addition of IR radiation prior to the VUV radiation: previously observed mass channel signal intensity increases and/or decreases with the added IR photons absorbed by various species in the beam.

A decrease of the mass spectral intensity for a cluster or its fragment with the addition of IR photons prior to the VUV photon implies that the original cluster has fragmented and that higher order multimers are not fragmenting substantially into this detected mass channel. An increase in the signal intensity of a given mass channel under these conditions implies that clusters of larger size are fragmenting into the detected mass channel and displaying their spectra on top of that of the original species in that mass channel. Thus spectra for a given cluster size can be reasonably well determined on the basis of the "sign" of the "ion-dip" detected in a specific mass channel.[19] Some monomer channels for various conformers could confuse this generalization but such species are not detected in this present cluster study.

We present herein the study of valine clusters, generated in a gas phase supersonic expansion, employing IR/VUV ion-dip spectroscopy.[19] The series of protonated valine clusters ($(valine)_{n-1}H^+$, n = 2 to ∼5) and other valine cluster related fragments are detected by time-of-flight mass spectrometry (TOFMS) following ionization by 118 nm photons. Absorption of IR radiation by neutral valine clusters prior to ionization is detected in the same mass channels. Both loss and gain of intensity are observed in different mass channels as the clusters and monomer absorb IR radiation in the CH, NH, and OH fundamental vibration region in the 2500−4000 cm^{-1} range. Structural information and some dynamics can be deduced about these clusters and are discussed on the basis of the observed IR spectra and model density functional theory (DFT) calculations.

II. Experimental Procedures and Computational Methods

The apparatus used to record VUV TOFMS and IR spectra has been described previously.[19] Valine is purchased from Aldrich and used without additional purification. The solid sample of valine is placed close to the valve body of a Parker General Valve Series 9 solenoid valve. In our previously published valine study, for which low valine vapor pressure was employed for the study of valine monomers, the temperature of the valve was lower than 200 °C. In the present studies, sample plus valve are heated to ca. 220 °C to generate enough concentration in the vapor phase (ca. 6 Torr) to form clusters in the supersonic expansion. At this temperature, the thermally fragile, low volatility valine molecules remain intact in the gas phase.[20] The gaseous amino acid molecules are seeded into a 70% Ne/30% He gas mixture at 2 atm total pressure, and expanded into the vacuum system through the above pulsed valve with a pulse width of ∼150 μs duration. After passing through a skimmer, the molecular beam interacts with pulsed IR and VUV light (ca. 10 ns), from two different lasers, in the ionization region of the TOFMS. The generated ions are detected in the TOFMS. The TOFMS has been set to maximize the intensity of the higher masses (i.e., cluster related signals) by

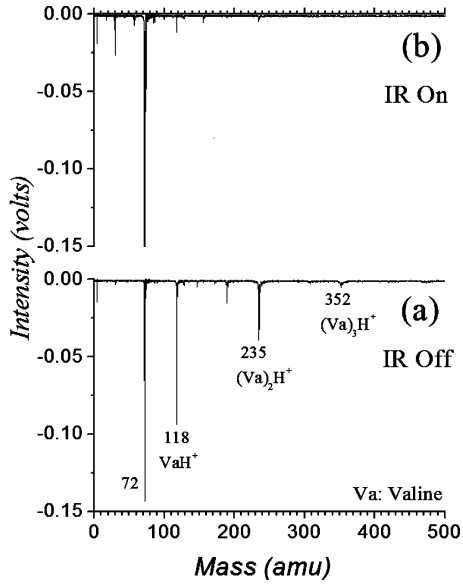

Figure 1. Time of flight mass spectrum for valine clusters formed in a supersonic expansion ionized by VUV (118 nm) single photons: bottom trace (a) obtained with IR/off; top trace (b) obtained with IR/on.

optimizing the time delay between the nozzle opening and the VUV laser triggering.

The light beams counterpropagate with respect to one another and are both perpendicular to the TOFMS flight tube axis and the molecular beam. The IR beam is focused upstream from the VUV/molecular beam interaction point at the center of the ionization region by a 40 cm focal length lens to access the neutral ground state species. Generation of the VUV light and IR light is similar to that described earlier.[19] The 118 nm VUV light is the ninth harmonic of the 1.064 μm fundament radiation of a Nd^{3+}/YAG laser. Radiation (355 nm) from a Nd^{3+}/YAG laser (third harmonic) is focused into a cell containing a Xe/Ar 1:10 mixture at 200 Torr total pressure. A MgF_2 lens focuses the 118 nm light in the ionization region of the TOFMS and disperses the remaining 355 nm light. Tunable IR radiation output in the mid-IR and near-IR range has a pulse energy of 3−5 mJ/pulse, a time duration of ~10 ns, and a bandwidth of ~2 cm^{-1}.

To predict structures and energies of the valine clusters and their fragment cations, we perform DFT calculations with the Gaussian 03W program package[22] at the B3LYP/6-31+G** level. Frequency calculations are employed to determine the nature of stationary points found by geometry optimization and to generate the zero point vibrational energies of the species.

III. Results and Discussion

Figure 1 presents the time-of-flight mass spectrum of valine generated under high temperature conditions such that the beam valine concentration is high. Figure 1a presents the mass spectrum of the valine sample with the IR laser off; Figure 1b presents the mass spectrum of the valine sample with the IR laser on (IR wavenumber at ~3000 cm^{-1}). Prominent features appear at 72 amu (valine monomer fragment),[24,25] 118, 235, 352, 469 amu ($(valine)_{n-1}H^+$, $n = 2-5$, fragments), and other mass channels (e.g., 147, 189, ... amu). The latter mass channels represent 117 + 30 and 117 + 72 amu, as expected for valine monomer fragmentation from a neutral dimer, trimer, tetramer, etc.

Recall that two sources of cluster dissociation and/or fragmentation exist: (1) cluster dissociation due to vibrational energy (due to IR photon absorption) added to the ground electronic state cluster prior to cluster ionization by a 118 nm photon and (2) ionization related fragmentation of both clusters and monomers associated with the difference between vertical and adiabatic ionization energies (VIE − AIE) plus the rearrangement reaction energy (ΔH) following the VIE transition. The second mechanism has been found for many van der Waals clusters,[19−21,26,27] and the first has been discussed for methanol and ethanol clusters.[19] Both mechanisms are found for van der Waals clusters, in general. Since cluster mass channels lose intensity upon IR absorption, the monomer fragment channels gain intensity with IR absorption, and IR spectra in cluster mass channels appear generally similar (but see below), we conclude that cluster dissociation (due to IR irradiation) occurs on the neutral ground electronic state surface of the clusters, although some fragmentation on the ion surface is certainly possible and cannot be completely excluded. Cluster fragmentation, that is, $(valine)_2^+ \rightarrow (valine)H^+ + X$ and $(valine)_2^+ \rightarrow (valine)Y^+ + Z$, occurs on the ground electronic state of the cluster ion, as discussed previously.[19j] For mass channels 147 and 189 amu, the species can be identified as $(valine)CH_2NH_2^+$ and $(valine)(NH_2)CHCH(CH_3)_2^+$. Mass channels 118, 235, 352, and 469 amu are $(valine)_{n-1}H^+$, $n = 2, 3, 4, 5$, respectively, and can be associated with the $(valine)_n$, neutral clusters, respectively, in the absence of IR radiation. IR spectra detected in the same mass channels can also be associated with neutral $(valine)_n$ clusters, because the IR absorption causes a decrease in the population of the respective detected mass channels. Since a cluster−monomer binding energy is ca. 2500 cm^{-1}, absorption of one or more IR photons can cause cluster dissociation on the ground state neutral cluster potential energy surface in ca. 100 ns. Additionally, the cluster ion−monomer binding energy is ca. 5000 cm^{-1}. Thus, under IR plus VUV (118 nm) irradiation, other clusters could contribute to these mass channels by losing one or more valine monomers, and thereby the IR spectrum of the monomer could be distorted. Our results reveal that the IR spectrum for the monomer does show such positive contributions from the clusters (see the broad feature between 2500 and 3500 cm^{-1}). Note that the fragmentation and dissociation reactions as observed in the mass spectra of Figure 1 are identical for both IR on and off conditions, and that the same is true for the monomer (fragment) mass spectra.[19,23] This kind of distortion does not dominate the cluster spectra because (1) concentrations of larger clusters are less than those of the smaller ones, (2) cluster excess vibrational energy is not very large, (3) IR radiation does not in general cause new fragments to appear, and (4) cluster spectra are in general negative. Nonetheless, the protonated valine cation at mass channel 118 amu, which is generated mainly from fragmentation of the dimer, could have minor contributions from dissociation of larger clusters ($n > 2$).

The feature corresponding to the valine parent ion is absent from Figure 1; as previously reported,[19j,23] a feature at 72 amu (among others) is observed instead. This feature can be assigned as $(CH_3)_2CHCH(NH_2)^+$, i.e., valine minus COOH. The mass 72 amu fragment arises from the neutral monomer precursor, while the protonated monomer is mostly generated from the neutral dimer precursor. Intensity for the mass 73 amu fragment, corresponding to COO loss with the extra hydrogen on the amino group, is small compared to that of the 72 amu feature. This implies that the 73 amu fragmentation channel is not the dominant one for the monomer fragmentation. Following ionization, the dimer, etc. undergo hydrogen translocation and RCOO fragmentation, which reduces the cluster energy suf-

ficiently such that further cluster fragmentation does not occur. This latter fragment is generated by single photon ionization under 118 nm radiation. The fragmentation occurs on the ion ground state following the rearrangement reaction for the ion, as discussed above,[26,27] in our previous paper,[19j] and by others.[23] The two peaks at 147 and 189 amu in Figure 1 are probably generated from a C−C bond fission reaction in the dimer following 118 nm VUV, single photon ionization, although more elaborate processes associated with higher clusters can also contribute to such features in the TOFMS. Monomer fragment masses of 30 and 72 amu (as reported previously for the monomer)[23,24] with a remaining valine monomer (117 + 30 and 117 + 72 amu) can be assigned to these two mass channels (i.e., 147 and 189 amu). Similar results are observed in our previous study of acetic acid clusters:[19h] in this instance, the fragment $(CH_3COOH)-COOH^+$ is considered to arise from the cleavage of the acetic acid dimer at the β-CC bond to generate $(CH_3COOH)-COOH^+ + CH_3$ following single photon ionization. Thus, in like manner, cation 189 amu can be generated from a loss of COOH following C−C bond cleavage of one of the two monomers in the valine dimer. Cation 147 amu can be generated again from the dimer by loss of $(CH_3)_2CH$ and CO_2 neutrals following α- and β- carbon bond cleavage of a valine monomer. In this process, a hydrogen/proton transfers from one monomer's hydroxyl or amino group along the dimer hydrogen bond network to generate an $NH_2CH_2^+$ (30 amu) moiety solvated by a valine monomer (117 amu). (See Figure 4.) Note that larger clusters could also contribute to these two fragments under IR plus VUV (118 nm) radiation, as suggested above.

For clusters larger than the dimer, only the $(valine)_{n-1}H^+$ ion fragmentation channel appears to be open. This suggests that the proton affinities (PA) of clusters $(valine)_n$, $n \geq 2$, are larger than that of the monomer. This reaction pathway for larger clusters has smaller barriers and probably a more negative ΔH_{react} than do the more complicated monomer fragmentation reactions found for the dimer.

The principle of IR plus VUV nonresonant ionization and fragmentation detection of the vibrational spectra of amino acid monomers and clusters is similar to that reported for the ethanol system. Note that the VUV photon energy (10.49 eV) is close to the vertical ionization energy (VIE ∼ 9−10.5 eV)[23] for all the amino acid monomers. As the IR laser is scanned to excite vibrational modes of the cooled ground state cluster species in the beam prior to the introduction of VUV light, the various ion mass channel intensities are monitored. If the monomer were the only amino acid species in the beam, the absorbed IR radiation would simply add to the total energy of the molecule upon ionization and fragment mass channel signals would be enhanced and reduced as reported previously.[19j]

The presence of clusters in the beam changes this interaction because the absorbed IR radiation (single or multiple photon absorption) can fragment the clusters before they are ionized. Thus, neutral $(valine)_n$, $n = 2-5$ will generate valine monomer and dimer, trimer, and/or tetramer ions, as appropriate: most likely, one monomer will be produced for each cluster accessed, but this is somewhat a function of how many IR photons are absorbed by each species. One can anticipate, however, that the monomer derived mass channels (the amino acids do fragment upon 118 nm ionization due to a rearrangement reaction in the ion[19j]) will increase in intensity, while the cluster derived mass channels will decrease in intensity as the IR radiation is absorbed by each species. Thus the IR spectra detected at the various mass channels may not exactly represent the anticipated cluster spectrum but should approximate it if

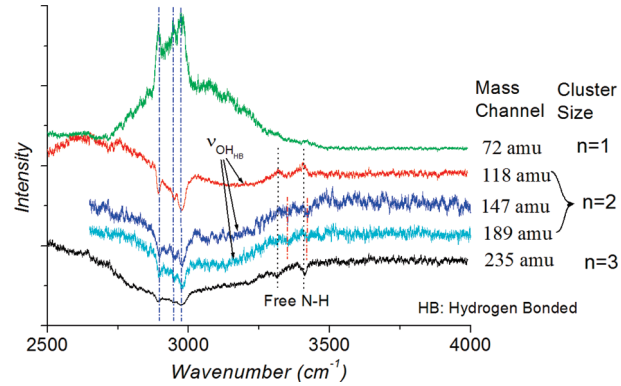

Figure 2. IR spectra for valine clusters $(valine)_n$ ($n = 1-3$) observed in the fragment mass channels as indicated. Note that 72 amu represents $NH_2CH-CH(CH_3)_2^+$, 147 amu represents valine$-NH_3CH^+$, 189 amu represents valine$-NH_2CH-CH(CH_3)_2^+$, 118 amu is the protonated monomer, and 235 amu is the protonated valine dimer. See text for more description and discussion of other possible cluster origins for some of the features.

the cluster concentrations follow a gas collision law. Even if most of the higher cluster species fragment into a lower cluster mass channel, the dominant signal detected in the lower mass channel should still be associated with the smaller cluster. This qualitative representation can be observed from Figures 1 and 2. The monomer spectrum, however, can be expected to be significantly distorted because all clusters should contribute a monomer to the appropriate mass channels for monomer fragments. This added population to the monomer species, due to cluster absorption and fragmentation, enhances the IR contribution to the monomer mass channel. As found previously,[19j] all ionized amino acids will fragment due to vertical/adiabatic ionization energy differences that drive the ion rearrangement reaction.

Figure 2 presents the mid-IR spectra of the high concentration neutral valine cluster system obtained by monitoring the mass channels $(valine)_nH^+$ ($n = 1,2$), and the fragment valine mass channels (valine) $(NH_2)CHCH(CH_3)_2^+$ (189 amu), $(valine)_1NH_2CH_2^+$ (147 amu), $NH_2CHCH(CH_3)_2^+$ (72 amu) while scanning the IR laser through the region 2500−4000 cm^{-1}. The top trace in this figure is detected in mass channel 72 amu: this spectrum is generated by free valine monomers not clustered in the beam, in addition to fragmented valine monomers derived from valine clusters dissociated by absorption of an IR photon(s).[19j] The latter monomer species bear the spectra of various clusters and thereby generate a composite valine monomer/cluster spectrum detected in mass channel 72 amu. As expected, this species generates "positive" TOFMS and IR spectra, as shown in Figure 2. And thereby, the other, cluster associated mass channels produce "negative" TOFMS and IR spectra. Some hint of "free" NH stretching modes can be seen in the 72 amu spectrum in the 3400 cm^{-1} region. The broad feature blending with the CH modes at ca. 3000 cm^{-1} and commencing at 3400 cm^{-1} is due to cluster OH and NH modes.[19] Apparently, some clusters fragment while others do not: the most likely cluster contribution to this monomer fragment channel (72 amu) is from the dimer, however, because of its more rapid dissociation and reasonably fast vibrational energy redistribution within the 10 ns IR pulse duration and because of its anticipated highest cluster concentration. Since all cluster mass channels (>117 amu) display similar, negative IR absorption signals and the monomer fragment mass channel 72 amu displays a positive IR absorption signal, we can conclude that the observed spectra in the $(valine)_{n-1}H^+$ mass channels

arise from the $(valine)_n$ neutral clusters. The cluster spectra are all similar and suggest that the OH moieties are involved in strong hydrogen bonds and that some of the NH_2 group hydrogens are not. Similar conclusions have been reached for fragmentation of other van der Waals and hydrogen bonded clusters.[19,20,27,28]

IR spectra for higher (>72 amu) mass channels in Figure 2 pertain to the neutral $(valine)_n$, $n = 2, 3, ...$ clusters. Note that nearly all of the features in these traces are negative, with the exception of the "free" NH modes in mass channel 118 amu. Thus, the neutral dimer, trimer, etc. lose population to the monomer due to IR absorption and their fragment mass channels decrease in intensity with IR irradiation. The dimer, etc. dissociation to the monomer, etc. occurs in the cluster neutral ground state, while the fragmentation to mass channels 72, 147, 189, ... amu occurs following ionization and rearrangement of the ionized species.[25,26] Thereby, a neutral tetramer cluster might absorb an IR photon (or two) at ca. 3000 cm^{-1}, generate a trimer, be ionized by a 118 nm photon, and then appear in the $(valine)_2H^+$ mass channel after rearrangement and fragmentation: this mechanism would account for the general set of observations of common IR spectra, and negative and positive IR on/off behavior of the TOFMS intensity for the different mass channels. Of course, other behavior could be possible, especially following 118 nm ionization, rearrangement, and more extreme cluster ion fragmentation (e.g., perhaps for 147 and 189 amu species). In any event, cluster IR spectra are "negative" in general (that is, IR absorption causes a decrease of the mass channel signal) so the observed cluster spectra are identified as belonging to the cluster detected in mass channel n, as indicated in Figure 2.

In the presence of IR radiation, fragments 118, 147, and 189 amu probably all arise from both neutral $(valine)_{2,3}$ clusters. As pointed out above, other higher clusters are also potential parent species but concentrations, energetics, and absorption probabilities do favor the neutral dimer route. See below for calculated dimer mechanisms. Nonetheless, the major IR spectra detected in these mass channels are related to the dimer.

Given this above probable mechanism for associating the spectra in mass channels 72 through 189 amu with various clusters, why are the NH spectral regions different as detected in these various mass channels? The features at 3318 and 3406 cm^{-1} that appear in the 118 amu mass channel can be assigned as due to "free" NH stretching modes of the neutral valine trimer (see Figure 2, intensity decrease in mass channel 235 amu).[7,8] Nonetheless, these features do not appear in other potentially neutral trimer related mass channels amu 147 and 189: instead, two very weak features (marked in Figure 2) are suggested as intensity decreases at ca. 3352 and 3424 cm^{-1}. The origin of these latter peaks can be related to a dimer. The fact that they are slightly blue-shifted with respect to the "free" N−H peaks in the 118 amu mass channel indicates the absence of the O−H···N hydrogen-bonding configuration in the structure. These peaks cannot be from the trimer or larger clusters. If they were, enhancements would have been observed. Another possibility is that intact valine monomers could fragment from an ion in the following reaction example: $(valine)_4 + IR \rightarrow (valine)_3^* + valine$, $(valine)_3^* + 118\ nm \rightarrow (valine)_3^{*+}$, $(valine)_3^* + \rightarrow (valine)_1X^+ + valine + Y$. We consider this latter fragmentation pathway less likely than the others suggested above because these ion generated monomers would not contribute to the spectrum presented in mass channel 72 amu. Thus, this latter pathway is probably not the major cluster ion fragmentation one. The "positive" NH_2 region contrasted with the "negative" OH and CH stretching regions can readily arise due to the composite nature of the spectra generated for this mass channel. For example, these NH_2 features may be associated with $(valine)_3$ while the other features may be associated with $(valine)_2$. Direct assignment of all the IR features is made difficult due to the possible dissociation/fragmentation pathways available to the clusters. Calculational efforts are presently underway that may address such issues.

All observed spectra (Figure 2) in the presented mass channels (Figure 1) show an intense broad feature between 2800 and 3400 cm^{-1}: for mass channel 72 amu this is a large increase in signal intensity and for the other mass channels it represents an equally intense decrease in mass channel signal. Previous studies of alcohols and organic acids, and of spectra of hydrogen bonded species in general,[19,29] reveal that such features are easily assignable to the hydrogen bond OH stretching modes interacting with CH, NH, and combination and overtone modes.[19,28,29]

Given the above analysis, one can conclude that $(valine)_n$ multimers with $n = 2-5$ are bonded by O−H···O and O−H···N hydrogen bonding, and that the NH symmetric and asymmetric stretch modes are not greatly perturbed by this interaction. These determinations are completely consistent with previous assignments and conclusions for other hydrogen bonded CH, NH, and OH groups containing molecules and clusters.[1−12,15−17,27,29] The structures of monomer conformers and clusters are easily based on free CH and NH group modes and hydrogen bonded O−H group modes.

On the basis of results for valine cluster and on previously studied hydrogen bonded species, we can model potential structures and fragmentation patterns for the valine dimer as an example of how such spectral patterns and fragments might arise. Three possible isomers for the valine dimer and their cations under these constraints are displayed in Figure 3. These structures are predicted at the B3LYP/6-31+G** level of theory. Two hydrogen O−H···O bonds are formed for isomer I, while two hydrogen O−H···N bonds are formed for isomer III. Isomer II, as presented in Figure 3, has one of each of these two hydrogen O−H bonds. The calculated predicted energies of these structures are given in Figure 3. Isomer I has the lowest energy, the energies of isomers II and III are higher by ca. 0.26 and 0.57 eV, respectively. The cation of isomer II tends to fragment and generate protonated valine with the proton on the amine group (isomer a), CO_2, and $R-CH-NH_2$ ($R = CH(CH_3)_2$); this fragmention pathway has a low barrier.

As an example of how such clusters might fragment, consider the dimer case as presented in Figure 3. The above-described trimer mechanism may still be more probable, but the dimer is more accurately calculated and should demonstrate the basic principles and ideas for a cation fragmentation mechanism. Single photon ionization and fragmentation reactions outlined in Figure 4 could occur for these dimers. The enthalpy values in electronvolts for these reaction pathways are calculated at the B3LYP/6-31+G** level of theory. Dimer isomer I can generate a $(valine)H^+$ (isomer b, Figure 4) with the extra proton (mass channel 118 amu) attached to the carboxylic group (see Figure 4, pathway *I-a*). The endothermic reaction energy for this pathway is ca. 9.58 eV, which is higher than the vertical ionization energy (VIE) of the dimer isomer I at ca. 8.55 eV (see Figure 3), but lower in energy than the 10.5 eV photon employed for ionization. This protonated valine with proton on the oxygen (isomer b, Figure 4) could also be generated by isomer II (Figure 4, pathway *II-a*), which requires at least 9.31 eV, higher than the VIE of the dimer (isomer II) at ca. 8.78 eV (see Figure 3). The protonated valine isomer with the proton

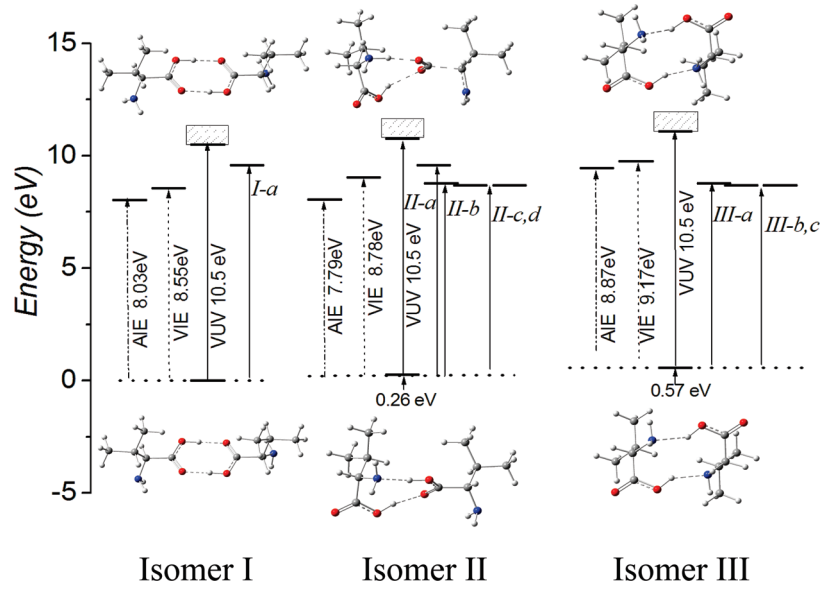

Figure 3. Relative energies of the species involved in the single photon ionization and fragmentation of the three valine dimer isomers under VUV (118 nm) radiation. Structures for the proposed three valine dimer isomers and their cations, predicted at the level of B3LYP/6-31+G**. Isomer I (2OHO) represents the valine dimer for which two hydrogen O−H···O bonds are formed; isomer II (NHO−OHO) represents the valine dimer for which hydrogen O−H···N and O−H···O bonds are formed; and isomer III (2NHO) represents the valine dimer for which two hydrogen N−H···O bonds are formed. See Figure 4 for details of the reaction pathways. The experimental temperature of the clusters is not known.

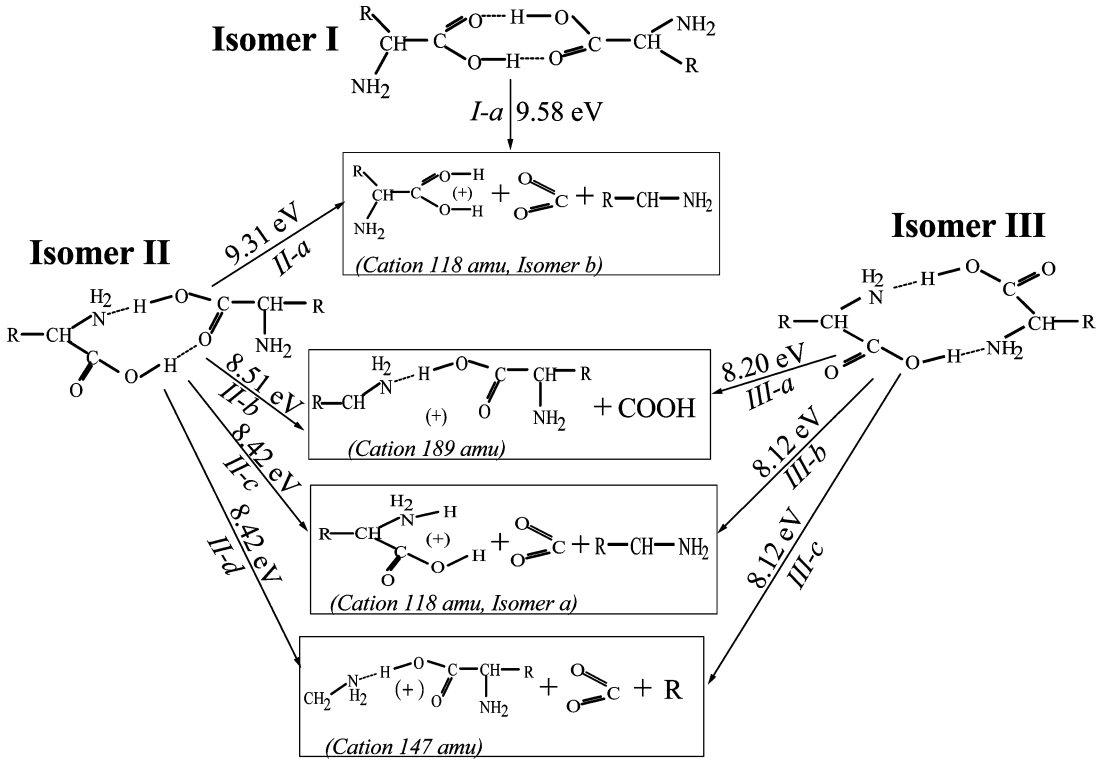

Figure 4. Scheme of possible fragmentation pathways of the valine dimer isomers under VUV (118 nm, 10.5 eV) radiation. Enthalpy values are given for the reactions. The valine dimer, the fragment cations, protonated valine isomer a and b, 147 amu, and 189 amu, predicted at the B3LYP/6-31+G** level of theory. (Valine)H_(N) (isomer a) represents protonated valine with the proton on the amino group and (Valine)H_(O) (isomer b) represents protonated valine with the proton on the carboxylic acid group. Isomer b is lower in energy than isomer a by 0.89 eV at the employed level of theory.

attached to the amino group (isomer a) can best be formed by photoionization and fragmentation of isomers II and III, considering only the most direct fragmentation pathways, *II-c* and *III-b*, which require at least ca. 8.42 and 8.12 eV added energy, respectively. The protonated isomer a (···NH_3^+) is determined to be the lower energy fragment conformer, on the basis of a previous report.[29] Our calculational results show that the energy of the protonated valine isomer b is higher (ca. 0.89 eV) than that of Isomer a at the calculation level of B3LYP/6-31+G**. Pathways *II-d*, *II-b*, and *III-c*, *III-a* in Figure 4 show that the cations 147 and 189 amu can be derived through single photon ionization of the dimer isomers II and III, followed by rupture of C−C bonds. Cation 189 amu can be formed by loss of COOH following simple rupture of the C−C bond linking the carboxyl group to the α-carbon of the valine after the dimers (II and III) are ionized, with the total endothermic energies of

ca. 8.51 eV for *II-b* and 8.20 eV for *III-a*, respectively. DFT calculations suggest that the generation of 189 amu fragment cations is through a multistep proton/hydrogen transfer reaction before reaching a stable geometry. Generation of the 147 amu cation requires additional cleavage, following a fast proton transfer reaction, of the C−C bond between the α- and β-carbons of valine and the bond linking the carboxyl group to the α-carbon of valine. The reaction enthalpies for the two pathways/generating cation 147 amu are, however, a little lower than those for generating 189 amu cations; these are 8.42 eV (*II-d*) and 8.12 eV (*III-c*), given in Figure 4. The trimer can be expected to have a number of isomers and its decomposition mechanisms will probably be more complicated in detail, even though the only observed feature that is directly associated with the trimer is $(val)_2H^+$.

These DFT calculations generate reaction enthalpies for the above fragmentation pathways that are lower by ca. 1−2 eV than the single VUV photon energy (10.5 eV), the VIE, and the rovibronic total energy in the clusters. Free energies would be the more relevant parameter, but the results would not change the conclusion because the calculational uncertainty at the B3LYP/6-31+G** level (ca. 4.0 kcal/mol)[30] is higher than the difference between the two quantities. Additionally, the cluster temperature is not well-defined for the ion and may not be a realistic parameter. Such results, however, only indicate that these fragmentation reactions are thermochemically accessible. The intensity ratios of the features representing these fragment cation channels in the mass spectra are not necessarily consistent with the reaction enthalpies for these reactions, because one or more barriers for these processes will exist, and the reactions must proceed through one or more transition states (TS), as well. The ratio of these TS energies, which can be expected to be lower than 10.5 eV will finally determine a pathways' probability and can be related to the ratio of the intensities of the features in the mass spectra. Ab initio, complete active space self-consistent field (CASSCF) calculations presently undertaken in our group are designed to address these dissociation mechanisms more completely, with special attention given to the different low lying accessible cluster ion states and their interactions at conical intersections.[13c]

IV. Conclusions

The data presented here constitute the first IR spectral measurement of a gas phase, neutral aliphatic amino acid cluster $(valine)_n$ (n = 2, 3, 4) series in the energy range 2500−4000 cm^{-1}. The combination of time-of-flight mass spectrometry and IR plus vacuum ultraviolet spectroscopy is employed to observe the infrared absorption spectra of the sequence of neutral valine clusters. A series of protonated valine clusters $(valine)_{n-1}H^+$ (n = 2−5) can be observed in the mass spectrum, which is generated by single photon, soft ionization of the neutral clusters $(valine)_n$ (n = 2−5) under 118 nm radiation. Absence of the free O−H stretching mode in the spectra of these clusters indicates that all the OH moieties are bonded in the clusters, while free NH stretching modes observed in the spectra suggest that the hydrogen atoms of the amino group are not directly involved in the hydrogen bonds holding the clusters together. Qualitative mechanisms for the chain of reactions taking neutral valine ground state clusters under IR irridation to protonated clusters, fragmented clusters, and fragment molecules are proposed and are supported by DFT calculations. These steps can be generally expressed as $(valine)_n + IR \rightarrow (valine)_{n-1} +$ valine; $(valine)_{n-1} + 118\ nm \rightarrow (valine)_{n-1}^+$; $(valine)_{n-1}^+ \rightarrow (valine)_{n-2}H^+ + Z$ and $(valine)_{n-2}X^+ + Y$; $valine + 118\ nm \rightarrow valine^+ \rightarrow X^+ + Y$. The valine cluster IR spectra are all generally negative in the sense that IR absorption decreases the cluster mass channel signal intensity. This observation implies that a loss of concentration has occurred for the involved cluster due to IR absorption. Thus, the particular IR spectrum detected in a given mass channel is related to the cluster whose mass is that of the next higher mass valine cluster. Specifically, detected ions (valine) H^+ and (valine) X^+ reveal the dimer IR spectrum, $(valine)_2H^+$ reveals the valine trimer spectrum, and $(valine)_3H^+$ reveals the valine tetramer IR spectrum, etc.

Acknowledgment. Dr. Yongjun Hu thanks Guadong-NSF grants (No. 7005823) and the start foundation for the outstanding talent scientist at SCNU (South China Normal University).

Supporting Information Available: Complete ref 22. This material is available free of charge via the Internet at http://pubs.acs.org.

References and Notes

(1) (a) de Vries, M. S.; Hobza, P. *Annu. Rev. Phys. Chem.* **2007**, *58*, 585. (b) Dian, B. C.; Clarkson, J. R.; Zwier, T. S. *Science* **2004**, *303*, 1169. (c) Dian, B. C.; Longarte, A.; Zwier, T. S. *Science* **2002**, *296*, 2369.
(2) Page, R. H.; Shen, Y.; Lee, Y. T. *J. Chem. Phys.* **1988**, *88*, 4621.
(3) Ebata, T.; Fujii, A.; Mikami, N. *Int. Rev. Phys. Chem.* **1998**, *17*, 331.
(4) Nir, E.; Janzen, C.; Imhof, P.; Kleinermanns, K.; de Vries, M. S. *J. Chem. Phys.* **2001**, *115*, 4604.
(5) Zwier, T. S. *J. Phys. Chem. A* **2006**, *110*, 4133.
(6) Abo-Riziq, B. C.; Grace, L.; de Vries, M. S. *J. Am. Chem. Soc.* **2005**, *127*, 2374.
(7) Snoek, L. C.; Robertson, E. G.; Kroemer, R. T.; Simons, J. P. *Chem. Phys. Lett.* **2000**, *321*, 49.
(8) Snoek, L. C.; Kroemer, R. T.; Hockridge, M.; Simons, J. P. *Phys. Chem. Chem. Phys.* **2001**, *3*, 1819.
(9) Jockusch, R. A.; Talbot, F. O.; Rogers, P. S.; Simone, M. I.; Fleet, G. W. J.; Simons, J. P. *J. Am. Chem. Soc.* **2006**, *128*, 16771.
(10) Stearns, J. A.; Boyarkin, O. V.; Rizzo, T. R. *J. Am. Chem. Soc.* **2007**, *129*, 13820.
(11) (a) Simons, J. P.; Jockusch, R. A.; Çarçabal, P.; Huenig, I.; Kroemer, R. T.; Macleod, N. A.; Snoek, L. C. *Int. Rev. Phys. Chem.* **2005**, *24*, 489. (b) Çarçabal, P.; Jockusch, R. A.; Huenig, I.; Snoek, L. C.; Kroemer, R. T.; Compagnon, I.; Oomens, J.; Simons, J. P. *J. Am. Chem. Soc.* **2005**, *127*, 11414.
(12) Nir, E.; Hunziker, H. E.; de Vries, M. S. *Anal. Chem.* **1999**, *71*, 1674.
(13) (a) Ai, H. Q.; Bu, Y. X.; Li, P.; Li, Z. Q. *J. Chem. Phys.* **2004**, *120*, 11600. (b) Tan, S. X.; Yang, J. L. *J. Chem. Phys.* **2007**, *126*, 141103. (c) Bhattacharya, A.; Bernstein, E. R. Unpublished results. (d) Hu, Y. J.; Bernstein, E. R. *J. Phys. Chem. A* **2009**, *113*, 639.
(14) (a) Price, J. M.; Crofton, M. W.; Lee, Y. T. *J. Chem. Phys.* **1989**, *91*, 2749. (b) Clarkson, J. R.; Baquero, E.; Shubert, V. A. et al. *Science* **2005**, *307*, 1443. (c) Aviles-Moreno, J.-R.; Demaison, J.; Huet, T. R. *J. Am. Chem. Soc.* **2006**, *128*, 10467. (d) Belau, L.; Wilson, K. R.; Leone, S. R.; Ahmed, M. *J. Phys. Chem. A* **2007**, *111*, 7562.
(15) Bakker, J. M.; Compagnon, I.; Meijer, G.; von Helden, G.; Kabelac, M.; Hobz, P.; de Vries, M. S. *Phys. Chem. Chem. Phys.* **2004**, *6*, 2810.
(16) Borst, D. R.; Roscioli, J. R.; Pratt, D. W.; Florio, G. M.; Zwier, T. S.; Muller, A.; Leutwyler, S. *Chem. Phys.* **2002**, *283*, 341.
(17) Nir, E.; Kleinermanns, K.; de Vries, M. S. *Nature* **2000**, *408*, 949.
(18) (a) Gerhards, M.; Unterberg, C.; Gerlach, A.; Jansen, A. *Phys. Chem. Chem. Phys.* **2004**, *6*, 2682. (b) Wu, R.; McMahon, T. B. *J. Am. Chem. Soc.* **2007**, *129*, 4865.
(19) (a) Hu, Y. J.; Fu, H. B.; Bernstein, E. R. *J. Phys. Chem. A.* **2006**, *110*, 2629. (b) Fu, H. B.; Hu, Y. J.; Bernstein, E. R. *J. Chem. Phys.* **2006**, *124*, 024302. (c) Fu, H. B.; Hu, Y. J.; Bernstein, E. R. *J. Chem. Phys.* **2005**, *123*, 234307. (d) Hu, Y. J.; Fu, H. B.; Bernstein, E. R. *J. Chem. Phys.* **2006**, *124*, 114305. (e) Fu, H. B.; Hu, Y. J.; Bernstein, E. R. *J. Chem. Phys.* **2006**, *125*, 014310. (f) Hu, Y. J.; Fu, H. B.; Bernstein, E. R. *J. Chem. Phys.* **2006**, *125*, 154306. (g) Hu, Y. J.; Fu, H. B.; Bernstein, E. R. *J. Chem. Phys.* **2006**, *125*, 154305. (h) Hu, Y. J.; Fu, H. B.; Bernstein, E. R. *J. Chem. Phys.* **2006**, *125*, 184308. (i) Hu, Y. J.; Fu, H. B.; Bernstein, E. R. *J. Chem. Phys.* **2006**, *125*, 184309. (j) Hu, Y. J.; Bernstein, E. R. *J. Chem. Phys.* **2008**, *128*, 164311.
(20) (a) Svec, H. J.; Clyde, D. D. *J. Chem. & Eng. Data* **1965**, *10*, 151. (b) Dong, F.; Heinbuch, S.; Rocca, J. J.; Bernstein, E. R. *J. chem. Phys.* **2006**, *124*, 24319. (c) Dong, F.; Heinbuch, S.; Rocca, J. J.; Bernstein, E. R.

J. Chem. Phys. **2006**, *125*, 154317. (d) Heinbuch, S.; Dong, F.; Rocca, J. J.; Bernstein, E. R. *J. Chem. Phys.* **2006**, *125*, 154316. (e) Heinbuch, S.; Dong, F.; Rocca, J. J.; Bernstein, E. R. *J. Chem. Phys.* **2007**, *126*, 244301. (f) Guo, Y. Q.; Bhattacharya, A.; Bernstein, E. R. *J. Phys. Chem. A* **2009**, *113*, 85. (g) Clawson, J. J.; Bhattacharya, A.; Shin, J. W.; Bernstein, E. R. "Decomposition of Photoionizaed Cationic Aliphatic Amino Acids", manuscript in preparation.

(21) (a) Lien, Y. C.; Nawar, W. W. *J. Food Sci.* **1974**, *39*, 911. (b) Dong, F.; Heinbuch, S.; He, S. G.; Xie, Y.; Rocca, J. J.; Bernstein, E. R. *J. Chem. Phys.* **2006**, *125*, 164318. (c) He, S. G.; Xie, Y.; Bernstein, E. R. *J. Chem. Phys.* **2006**, *125*, 164306. (d) He, S. G.; Xie, Y.; Guo, Y.; Bernstein, E. R. *J. Chem. Phys.* **2007**, *126*, 194315. (e) He, S. G.; Xie, Y.; Dong, F.; Heinbuch, S.; Jakubikova, E.; Rocca, J. J.; Bernstein, E. R. *J. Phys. Chem. A*, in press. (f) Dong, F.; Heinbuch, S.; Xie, Y.; Rocca, J. J.; Wang, Z.; Deng, K.; He, S. G.; Bernstein, E. R. *J. Am. Chem. Soc.* **2008**, *130*, 1932.

(22) Frisch, M. J.; et al. *Gaussian 03*, revision C.02; Gaussian, Inc.: Wallingford, CT, 2004.

(23) Jochims, H. W.; Schwell, M.; Chotin, J. L.; Clemino, M.; Dulieu, F.; Baumgärtel, H.; Leach, S. *Chem. Phys.* **2004**, *298*, 279.

(24) Lago, A. F.; Coutinho, L. H.; Marinho, R. R. T.; Naves de Brito, A.; de Souza, G. G. B. *Chem. Phys.* **2004**, *307*, 9.

(25) Fanourgakis, G. S.; Shi, Y. J.; Consta, S.; Lipson, R. H. *J. Chem. Phys.* **2003**, *119*, 6597.

(26) Oomens, J.; Sartakov, B. G.; Meijer, G.; von Helden, G. *Int. J. Mass Spectrom.* **2006**, *254*, 1.

(27) Mirkin, N. G.; Krimm, S. *J. Phys. Chem. A* **2004**, *108*, 5438.

(28) Kozich, V.; Dreyer, J.; Ashihara, S.; Werncke, W.; Elsaesser, T. *J. Chem. Phys.* **2006**, *125*, 074504.

(29) El Aribi, H.; Orlova, G.; Hopkinson, A. C.; Siu, K. W. M. *J. Phys. Chem. A* **2004**, *108*, 3844.

(30) Foresman, J. B. Frisch, A. *Exploring Chemistry with Electronic Structure Method*, 2nd ed.; Gaussian, Inc.: Wallingford, CT, 1996.

JP901208F